NÖHÜ Müh. Bilim. Derg. / NOHU J. Eng. Sci., 2025; 14(1), 308-317

Niğde Ömer Halisdemir Üniversitesi Mühendislik Bilimleri Dergisi
Niğde Ömer Halisdemir University Journal of Engineering Sciences

Araştırma makalesi / Research article

www.dergipark.org.tr/tr/pub/ngumuh / www.dergipark.org.tr/en/pub/ngumuh

Tracking seasonal coastal dynamics of Ağyatan wetland using object-based Classification and Regression Tree

Nesne tabanlı Sınıflandırma ve Regresyon Ağacı kullanılarak Ağyatan sulak alanının mevsimsel kıyı dinamiklerinin izlenmesi

Mustafa Hayri Kesikoğlu[1], Tolga Kaynak[2,*]

[1] *Uşak University, Civil Engineering Department, 64000, Uşak, Türkiye*
[1] *Uşak University, Urban and Regional Planning Department, 64000, Uşak, Türkiye*
[2] *Niğde Ömer Halisdemir University, Geomatics Engineering Department, 51240, Niğde, Türkiye*

Abstract

In recent years, the management of water and wetlands has become increasingly important. Ağyatan Wetland is a natural lake formed by the Ceyhan River, located west of the river. The area around the wetland is home to various sea and land creatures, as well as endemic plants and endangered birds. This study aimed to analyze the seasonal changes occurring in the Ağyatan wetland in 2016. Landsat 8 images from four seasons of 2016 were utilized to identify these changes. The study areas were classified into six categories: lake, sea, cultivated agricultural land, barren land, building area, and water channel. Thematic maps for the four seasons were generated using the object-based Classification and Regression Tree (CART) method. Additionally, change detection analyses were conducted using the post-classification comparison method. The study revealed a decrease in the lake area from winter to spring (0.8919%), followed by an increase from spring to summer (0.3627%) and summer to autumn (0.1953%) in 2016. This fluctuation was attributed to groundwater, river water, and melting snow.

Keywords: Change detection, Object-based classification, CART, Wetland, Landsat 8

Öz

Son yıllarda su ve sulak alanların yönetimi giderek önem kazanmıştır. Ağyatan Sulak Alanı, Ceyhan Nehri'nin batısında yer alan doğal bir göldür. Sulak alan çevresi çeşitli deniz ve kara canlılarına, endemik bitkilere ve nesli tükenmekte olan kuşlara ev sahipliği yapmaktadır. Bu çalışmada, 2016 yılında Ağyatan Sulak Alanı'nda meydana gelen mevsimsel değişimlerin analizi amaçlanmıştır. Bu değişimlerin belirlenmesi için 2016 yılının dört farklı mevsimine ait Landsat 8 görüntüleri kullanılmıştır. Çalışma alanları göl, deniz, ekili tarım arazisi, çıplak alan, yapı alanı ve su kanalı olmak üzere altı kategoriye ayrılmıştır. Dört mevsime ait tematik haritalar, nesne tabanlı Sınıflandırma ve Regresyon Ağacı (CART) yöntemi kullanılarak üretilmiştir. Ayrıca, sınıflandırma sonrası karşılaştırma yöntemi kullanılarak değişim tespiti analizleri yapılmıştır. Çalışmada, 2016 yılında göl alanında kıştan ilkbahara doğru (0.8919%) bir azalma, ardından ilkbahardan yaza (0.3627%) ve yazdan sonbahara (0.1953%) doğru bir artış olduğu ortaya konulmuştur. Bu dalgalanmanın yeraltı suyuna, nehir suyuna ve eriyen karlara bağlandığı belirtilmiştir.

Anahtar kelimeler: Değişim belirleme, Nesne tabanlı sınıflandırma, CART, Sulak alan, Landsat 8

1 Introduction

Recently, remote sensing has become one of the most preferable disciplines to conduct land use/land cover detection, wetland management, ecological studies, and monitoring of deformations. Images obtained by remote sensing discipline produce useful results with the classification process. There are two commonly utilized classification approaches namely object-based and pixel-based classifications. Pixel-based classification is made by using the spectral information of each pixel. However, pixel groups are used in the object-based classification method. Object-based classification is used as an alternative to the pixel-based classification method. In object-based classifications, some properties such as size, shape, and texture of pixel groups are examined and the analysis is based on these segments. Also, properties such as location and coexistence are questioned in object-based classifications [1]. In the literature, there are some studies about the comparison of object-based and pixel-based classification. Gholoobi et al. [2] performed pixel-based and object-based classification to determine land use/land cover in mountainous regions, and object-based classification gave more accurate results. Kalkan and Maktav [3] compared pixel-based and object-based classification on a 2x2 km area. Erdas software for pixel-based classification and eCognition software for object-based classification were used. Classification results were different from each other and object-based classification had also high accuracy. Therefore, the object-based classification method was used to provide high accuracy in classification. Recent studies have generally focused on highlighting the strengths and weaknesses of each approach in various applications. A notable study by Wang, (2023) [4] examined land use and

* Sorumlu yazar / Corresponding author, e-posta / e-mail: tolgakaynak@ohu.edu.tr (T. Kaynak)
Geliş / Recieved: 01.10.2024 Kabul / Accepted: 24.12.2024 Yayımlanma / Published: 15.01.2025
doi: 10.28948/ngumuh.1559034

land cover (LULC) changes in a subtropical region of South Africa, comparing the accuracy of pixel-based and object-based classification methods. The findings revealed that object-oriented classification consistently outperformed pixel-based methods. The study underscores the effectiveness of object-based approaches in capturing complex land cover features that pixel-based methods may overlook. Similarly, Aghababaei et al. (2021) [5] assessed the classification of plant ecological units in heterogeneous semi-steppe rangelands using Minimum Distance, Maximum Likelihood (ML), Artificial Neural Network (ANN)-Multi Layer Perceptron, and Classification Tree (CT) methods to compare pixel-based and object-based methods. The object-based CT method yielded superior accuracy in complex landscapes. The study emphasized that the spatial context provided by object-based methods allows for a more nuanced understanding of land cover types, which is particularly beneficial in heterogeneous environments. In another study, Turissa et al. (2021) [6] evaluated change detection methods for seagrass beds, highlighting the limitations of pixel-based ML classification, which primarily relies on spectral information. In contrast, it was indicated that the object-based image analysis (OBIA) method incorporates spatial dimensions through image segmentation, resulting in improved classification accuracy. Tonyaloğlu et al. (2021) [7] confirmed that object-based classification methods provide a more coherent representation of land cover types, particularly in high-resolution satellite imagery. Qu et al. (2021) [8] also contributed to this discourse by exploring the accuracy improvements in LULC classification through the use of auxiliary datasets in both pixel-based and object-based methods. They found that while pixel-based classification has been the focus of much previous research, object-based approaches are gaining traction due to their ability to integrate additional contextual information, leading to enhanced classification outcomes.

The coastline represents the boundary between land and water, but it becomes undefined in certain situations, such as during floods. The coastline can occasionally change due to seasonal events. Coastal research is a significant component in some areas such as coastal protection, wetland management, sea-level rise monitoring, land subsidence, and erosion-sedimentation [9]. Wetlands and wetland management are significant topics for remote sensing studies. In the literature, there are some studies about wetlands. Modi et al. [10] observed changes in the Kosi River affected by a flood. They detected land use/land cover changes using object-based classification and analyzed the flood in the wetland. Badjana et al. [11] determined land cover changes in the Binah River Basin using object-based classification of Landsat images. They also created land use maps. Sánchez-García et al. [12] observed coastal changes in the Gulf of Valencia by using four high-precision shoreline data and eleven Landsat images from 2006 to 2010 and achieved high accuracy. Recent studies have explored various machine learning algorithms for wetland classification, demonstrating the effectiveness of different approaches in accurately identifying and mapping these critical ecosystems. Lin et al. (2023) [13] utilized semantic segmentation techniques based on Sentinel-2 imagery, showcasing the advantages of machine learning algorithms over traditional classification methods in coastal wetland mapping. Similarly, Gonzalez-Perez et al. (2022) [14] employed deep learning and machine learning techniques on multispectral images obtained from unpiloted aircraft systems, highlighting the potential of these methods for detailed wetland vegetation mapping. In another study, Zhou et al. (2021) [15] implemented OBIA combined with machine learning algorithms to classify wetland vegetation, demonstrating the efficacy of this approach in handling complex data structures. Moreover, Adeli et al. (2021) [16] focused on the application of synthetic aperture radar (SAR) data in conjunction with machine learning techniques for wetland inventory mapping, emphasizing the robustness of these algorithms in delineating herbaceous wetland classes. Kesikoglu et al. (2019) [17] compared the performance of ANN, SVM, and ML algorithms for land use / cover change mapping in wetland areas, underlining the success of support vector machine (SVM). Similarly, Festus et al. (2020) [18] compared the performance of k-nearest neighbors (K-NN) and SVM algorithms in urban wetland classification, revealing the strengths of each method in different contexts. Çiftçi et al. (2024) [19] analyzed the impacts of land use and climate change on the Sugla water storage area in Turkey, emphasizing the importance of accurate land cover classification to capture the dynamic changes in wetland environments accurately.

One prominent approach is using a Classification and Regression Tree (CART) algorithm. The study by Feng et al. (2021) [20] highlighted the computational efficiency of CART, although it primarily focused on other classification methods and their applications in wetland distribution. Simioni et al. (2020) [21] compared CART with artificial neural networks (ANN) for detecting inland marshes, highlighting its reliability in wetland mapping. Similarly, Mahdianpari et al. (2020) [22] utilized CART with Google Earth Engine to create a high-resolution wetland inventory map, showcasing its capability to handle large datasets effectively. In another study, Gxokwe et al. (2022) [23] leveraged CART within the Google Earth Engine platform to characterize small seasonal wetlands, emphasizing its utility in semi-arid environments. These studies collectively underscore the versatility and effectiveness of the CART method in various wetland classification contexts, particularly when integrated with advanced remote sensing technologies. All the studies in the literature show that object-based classification methods and also the CART algorithm give successful classification results.

This study aims to perform object-based image classification with the CART method on the Ağyatan wetland area and also to compare the coastline changes of the wetland area in Adana, Turkey with the analysis of Landsat 8 Landsat Data Continuity Mission (LDCM) imagery.

2 Material and methods

2.1 *Study area*

Ağyatan wetland area is located in the Eastern Mediterranean Basin and near the Karatas, Adana [24]. It is located between land and sea as shown in Figure 1. Therefore, the lake can be influenced by factors of both terrestrial and marine ecosystem.

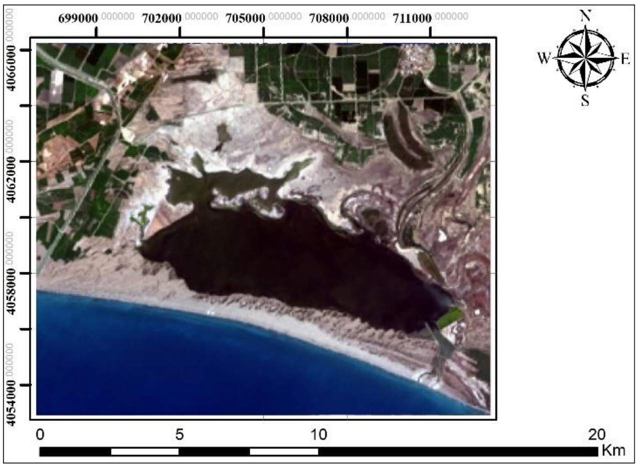

Figure 1. Landsat 8 LDCM image on February 2016 of the Ağyatan wetland area

The wetland area is the crossroads of migratory birds' migration routes. Different bird species live in the Ağyatan wetland area. There are also some endangered plants in this region [25]. For this reason, the Ağyatan wetland area is significant for natural life. The protection of the wetland is necessary not only for the maintenance of natural life but also for the sustainability of economic activities such as agriculture, fishing and tourism. Furthermore, the limited number of comprehensive studies in literature such as seasonal LULC or coastal dynamics analysis addressing the Ağyatan wetland makes this study even more meaningful. Therefore, following the seasonal changes in the wetland is very important.

2.2 *Material*

Four Landsat 8 Operational Land Imageries (OLI) having 30-meter spatial resolution are used to determine seasonal land use/cover classes in the study area for 2016 (Table 1). The Landsat 8 image used in the study was provided by United States Geological Survey (USGS) website [26]. Table 1 provides a detailed overview of the Landsat 8 bands, including their wavelengths and resolution values.

Table 1. Landsat 8 imagery image acquisition dates, cloud cover percentage and scene identifier

Date acquired	Landsat scene identifier	Cloud cover
26/02/2016	LC81750352016057LGN01	0.62
16/05/2016	LC81750342016137LGN01	2.91
20/08/2016	LC81750342016233LGN01	1.18
24/11/2016	LC81750352016329LGN02	0.27

Table 2. Landsat 8 bands and their wavelength and resolution [27]

Band	Wavelength (micrometers)	Resolution (meters)
Band-1 Ultra Blue (Coastal Aerosol)	0.43-0.45	30
Band-2 Blue	0.45-0.51	30
Band-3 Green	0.53-0.59	30
Band-4 Red	0.64-0.67	30
Band-5 Near Infrared (NIR)	0.85-0.88	30
Band-6 Shortwave Infrared (SWIR-1)	1.57-1.65	30
Band-7 Shortwave Infrared (SWIR-2)	2.11-2.29	30
Band-8 Panchromatic	0.50-0.68	15
9 Cirrus	1.36-1.38	30
Band-10 Thermal Infrared (TIRS-1)	10.60-11.19	100*30
Band-11 Thermal Infrared (TIRS-2)	11.50-12.51	100*30

2.3 *Methods*

The classification of the satellite image of the Ağyatan wetland and the change detection analysis are the two main steps of this research. The classification step consists of geometric correction (image recording), multiresolution segmentation and classification. Change detection analysis was done using the post-classification comparison method. Geometric correction and change detection analysis were performed in ENVI software, while multi-resolution segmentation and classification stages were performed in eCognition software.

2.3.1 *Geometric correction*

Geometric correction is the process of putting the image on a geographic coordinate system defined using ground control points. This operation aims to eliminate the effect of geometric distortion in a raw image [28].

2.3.2 *Multiresolution segmentation*

The multiresolution segmentation algorithm is a joining technique that is upward from below. Individual pixels aggregate into increasingly larger segments at multiple levels. It is a recursive process according to three parameters: scale, shape, and compactness [29]. This method defines single-image objects and combines pixels with neighbors according to the homogeneity criterion. These homogeneous criteria are a combination of spectral and shape measures.

2.3.3 *Classification and Regression Tree*

Classification and Regression Tree (CART) is a machine learning algorithm based on decision trees. This algorithm creates a tree structure that divides data according to its features and predicts the results with successive decisions (Figure 2). In this tree structure, the root node at the top represents the entire population, and each internal node represents data samples separated according to the values of the features. The subset creation process is repeated until a certain depth or a predetermined stopping criterion is reached [30]. While performing this process, the Gini index given in Equation (1) is used to determine each split point.

After this stage, the leaf nodes that make the final decision are obtained.

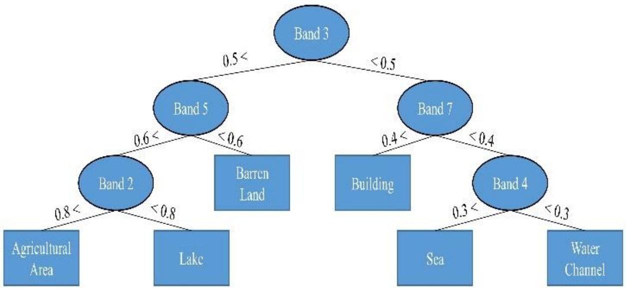

Figure 2. An example of a CART decision chart

$$g(t) = 1 - \sum_{i=1}^{c} p_i^2 \tag{1}$$

Where p_i represents the probability of the node splitting for the i number of classes and c represents the number of classes. The minimum of $g(t)$ values calculated separately for the threshold values consisting of the values of the initial feature is accepted as the threshold value for that feature and this process is repeated for the other features.

2.3.4 *Accuracy assessment and change detection*

The evaluation of the accuracy of classified images is conducted to assess the quality of the information obtained from the data [28]. For assessing the accuracy of land cover maps derived from satellite imagery, the stratified random sampling technique was applied to represent the various land cover classes in the region.

The fundamental logic in change detection analysis involves finding corresponding locations in two or more satellite images of the same geographical area and identifying dissimilar areas. Numerous approaches are utilized to detect change [31,32]. The change in the Ağyatan wetland area is obtained using the post-classification comparison method in this study. In employing this approach, it becomes feasible to precisely delineate both the specific land cover categories in which alterations take place and the corresponding magnitudes of these changes [33, 34].

3 Results and discussion

As part of the study, accurate, reliable, and expeditiously informative Landsat 8 satellite images representing four distinct seasons were employed as input data. The CART method was utilized to establish the delineation of lake area boundaries corresponding to each of these datasets. Benefiting from its marked sensitivity to spectral reflection values, this method has facilitated the extraction of intricate object details, yielding successful outcomes. The comprehensive methodology employed in this study is presented in Figure 3.

In this study, Landsat images were georeferenced to the Universal Transverse Mercator (UTM) projection system for images one-to-one overlap.

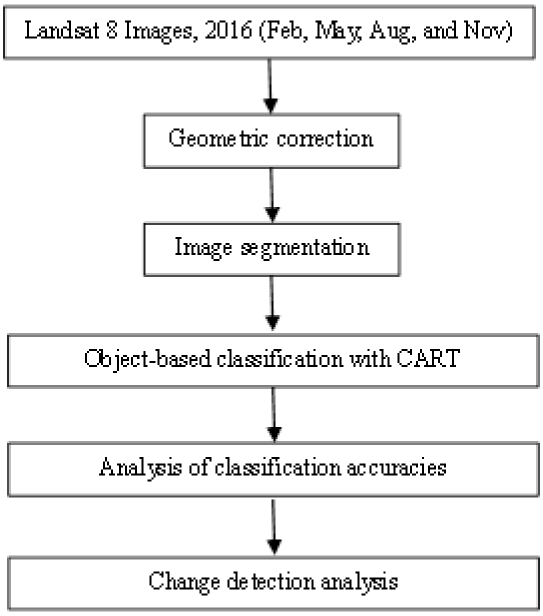

Figure 3. Flowchart of the study

For the geometric correction process, 48 Ground Control Points (GCP) distributed homogeneously over the images were used. The nearest neighbor resampling method was used for image rectification. The Root Mean Square Error (RMSE) for February, May, August, and November images were obtained 0.22, 0.19, 0.24, and 0.27 pixels, respectively.

In the first step, images were cropped to detect the study area, and multiresolution segmentation was performed on the study area images. Segmentation is a very critical stage in the process of creating a specific thematic map. This stage enables us to define each class by bringing together similar features in the image. Chessboard, one of the segmentation types, leads to loss of information in heterogeneous regions due to fixed-sized square cells. Although Quadtree is more flexible than the chessboard method, it prevents the accurate modeling of natural patterns because the shape of the objects is only square. In contrast, the multiresolution segmentation combines spectral and spatial features by the homogeneity criteria, thereby creating more natural boundaries and objects. This is a critical advantage for increasing the accuracy of LULC maps and provides a fundamental justification for the selection of our method. In this context, the selection of shape, scale and compactness parameters of the multiresolution method has a significant effect on the success of the classification.

The scale parameter determines the size of the objects. A smaller scale creates smaller and more detailed objects, while a larger scale creates larger and less detailed objects. To increase the accuracy of the resulting maps, a range of scale values between 10 and 500 were tried during segmentation and it was decided to use a scale value of 100 in the study. This value provided sufficient separation of the terrain classes, while at the same time not creating overly divided objects. The shape parameter determines the balance between colour and shape features. A low shape value gives more weight to colour information. Therefore, since the spectral differences between classes may be small, it was found that spectral features should be emphasized by using lower shape values. In this case, the shape parameter was selected as 0.1. The compactness parameter controls how compact (smooth) the objects will be. Lower compactness values lead to more irregular, natural boundaries; higher compactness values lead to smooth, compact object formation. Therefore, the compactness value was taken as 0.5 in the study. The resulting segmentation images for February, May, August and November are presented in Figures 4-7, respectively.

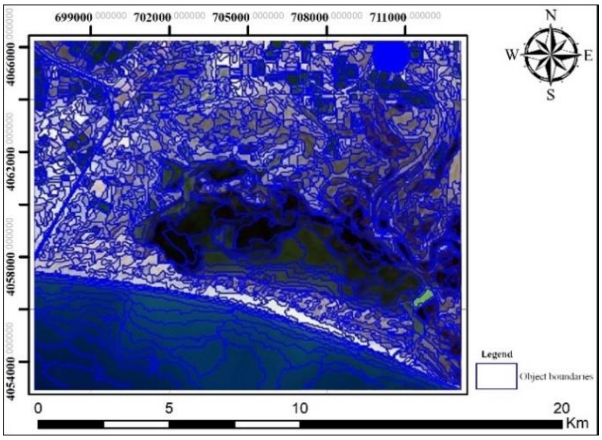

Figure 4. February segmentation image

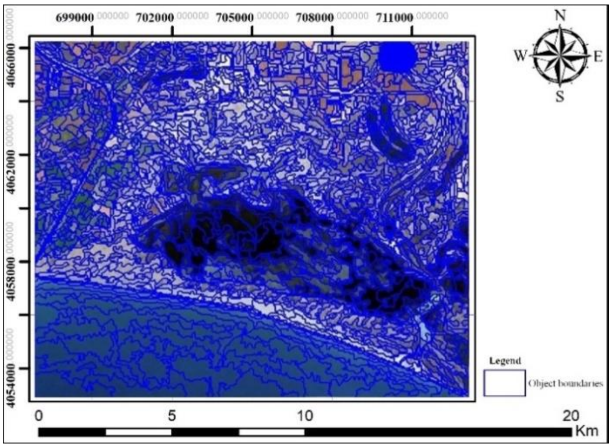

Figure 5. May segmentation image

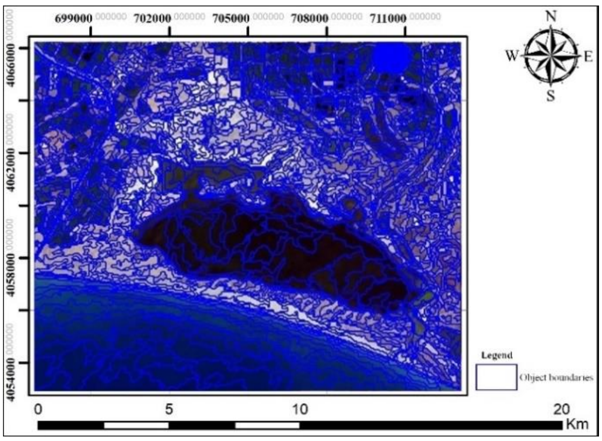

Figure 6. August segmentation image

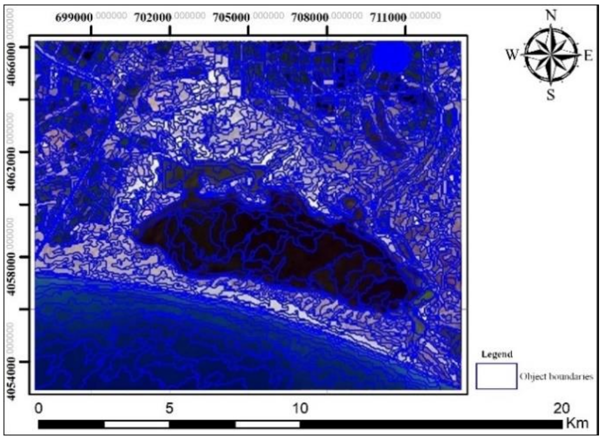

Figure 7. November segmentation image

In the second step, image classification was done by using the CART method. To carry out this process, objects containing approximately 7,000 pixels in total were selected for the classes of lake, sea, cultivated agricultural area, barren land, building area, and water channel. The number of pixels of each class was determined according to its percentage in the total area. Furthermore, the Google Earth platform was employed during the selection process.

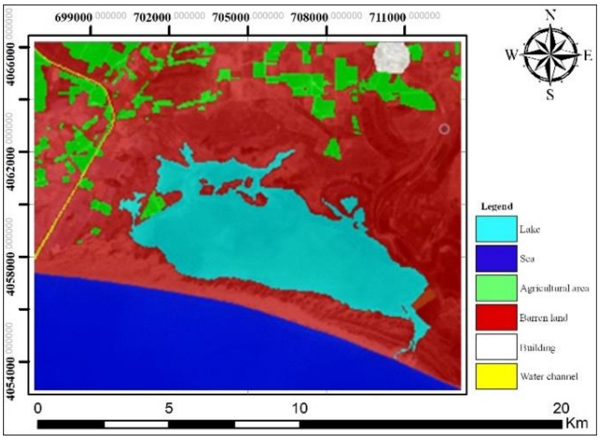

Figure 8. February segmentation image

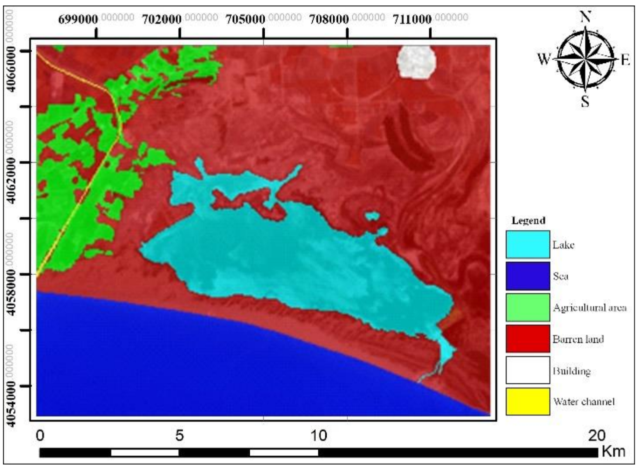

Figure 9. May segmentation image

The selected objects containing approximately 4,900 pixels were used in the training phase of the CART method. Additionally, spectral features (mean and brightness), indices (NDWI, NDVI and) and geometric features (elliptic fit, rectangular fit and roundness) were also selected during the classification phase. The study areas were classified into 6 classes: lake, sea, cultivated agricultural area, barren land, building area, and water channel. Thematic maps of four images were obtained as a result of the classification (Figure 8-11).

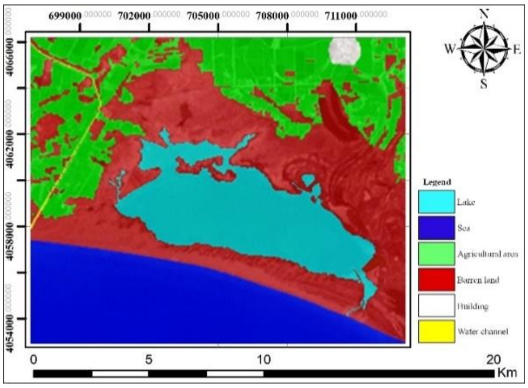

Figure 10. August segmentation image

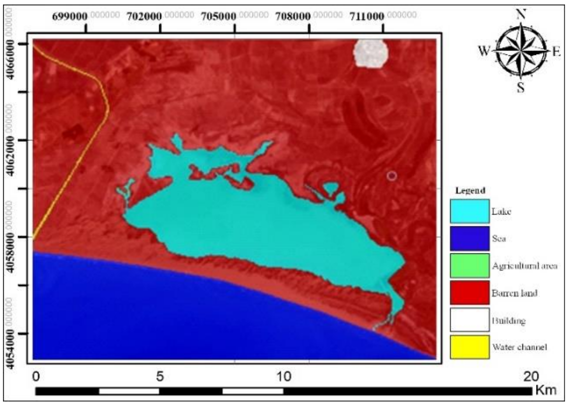

Figure 11. November segmentation image

In the third step, confusion matrices were created by overlapping the objects containing approximately 2100 pixels separated as test data with the classified images. These matrices were given for February, May, August and November, respectively (Table 3-6).

Table 3. Confusion matrix of February

	C1	C2	C3	C4	C5	C6		User (%)
Water channel (C1)	169	0	0	0	0	0	169	100
Building (C2)	0	242	0	0	0	0	242	100
Sea (C3)	0	0	305	0	0	0	305	100
Lake (C4)	0	0	0	341	7	0	348	98
Barren land (C5)	0	0	0	0	481	21	502	96
Agricultural (C6)	0	0	0	0	41	447	488	92
	169	242	305	341	529	468	2054	
Producer (%)	100	100	100	100	91	96		
Overall accuracy (%)		96.64						

Table 4. Confusion matrix of May

	C1	C2	C3	C4	C5	C6		User (%)
Water channel (C1)	169	0	0	0	0	0	169	100
Building (C2)	0	242	0	0	0	0	242	100
Sea (C3)	0	0	289	0	0	0	289	100
Lake (C4)	0	0	0	313	0	0	313	100
Barren land (C5)	0	0	0	0	530	0	530	100
Agricultural (C6)	0	0	0	0	33	544	577	94
	169	242	289	313	563	544	2120	
Producer (%)	100	100	100	100	94	100		
Overall accuracy (%)		98.44						

Table 5. Confusion matrix of August

	C1	C2	C3	C4	C5	C6		User (%)
Water channel (C1)	169	0	0	0	0	0	169	100
Building (C2)	0	242	0	0	0	0	242	100
Sea (C3)	0	0	276	0	0	0	276	100
Lake (C4)	0	0	5	314	0	0	319	98
Barren land (C5)	0	0	0	0	558	36	594	94
Agricultural (C6)	0	0	0	0	21	565	586	96
	169	242	281	314	579	601	2186	
Producer (%)	100	100	98	100	96	94		
Overall accuracy (%)		97.16						

Table 6. Confusion matrix of November

	C1	C2	C3	C4	C5		User (%)
Water channel (C1)	169	0	0	0	0	169	100
Building (C2)	0	242	0	0	0	242	100
Sea (C3)	0	0	338	0	33	371	91
Lake (C4)	0	0	0	283	0	283	100
Barren land (C5)	0	0	0	0	965	965	100
	169	242	338	283	998	2030	
Producer (%)	100	100	100	100	97		
Overall accuracy (%)		98.37					

When Table 3-6 is examined, it is seen that the classification accuracies are over 95%. Thus, it is understood that the classifications have high accuracies.

In the fourth step, the change in the Ağyatan wetland is acquired using the post-classification comparison method. According to these analyses, a decrease from the winter season to the spring, an increase from spring to summer, and summer to autumn were detected in the lake area. Changes which were a 0.8919% decrease from February to May, a 0.3627% increase from May to August, and a 0.1953% increase from August to November were determined. It has been determined that lake areas obtained from four distinct images exhibit varying responses to seasonal changes.

According to the World Meteorological Organization (WMO), 2016 was one of the hottest years on record, and this particularly affected water resources and wetland ecosystems. Due to the effects of El Niño events, extreme drought was observed in some regions and heavy rainfall was observed in some regions. This anomaly caused significant changes in the water level and ecosystem dynamics of wetlands. Therefore, seasonal changes in the study area in 2016 were monitored. To investigate the underlying reasons for seasonal changes, the temperature and precipitation values of the region were examined. Mediterranean region's annual precipitation belonging to Karatas/Adana is shown in Figure 12. According to the graphic, precipitation is approximately 87 mm in February, 49 mm in May, 6 mm in August, and 65 mm in November. It is seen that the temperature data is inversely proportional to the precipitation data in Figure 12. High rainfall increases the amount of water feeding the lake and causes the lake area to expand. High temperatures argue the opposite. In addition, the observed high temperatures increase evaporation rates, which in turn causes the lake area to decrease. These situations explain why the study area reaches its maximum area in February, the lake area decreases from winter to spring and the lake area increases from summer to autumn.

The coastline does not only change with precipitation, temperature and evaporation factors, but can also change with irrigation and natural factors. Spring is a period when irrigation activities are intensified because it is the planting and growing season. While spring irrigation activities consume more groundwater, in summer months, the sources that feed the lake may have recovered. In addition, the water holding capacity of the soil may be full in spring due to heavy precipitation and low temperatures. For this reason, some of the water may slowly leak into the lake in early summer, causing the lake level to rise. The increase in lake area from spring to summer is related to these situations.

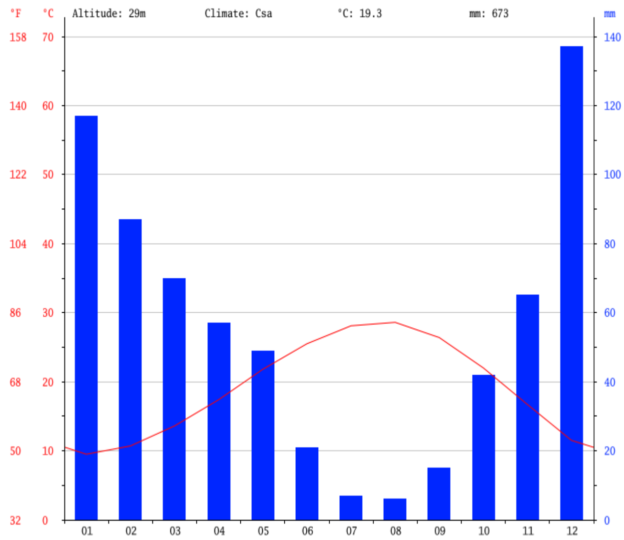

Figure 12. Mediterranean Region's annual precipitation and temperature graphic [35]

Overall, the comparative analysis of object-based and pixel-based classification methods reveals a clear trend favoring object-based approaches, particularly in complex and heterogeneous landscapes such as wetlands [4-8]. The ability of object-based methods to incorporate spatial relationships and contextual information significantly enhances classification accuracy, making them a valuable tool in remote sensing applications.

CART has been recognized for its interpretability and simplicity, making it a valuable tool in specific applications. In some comparative studies for mapping wetlands or land use / land cover areas [36-40], the authors evaluated the performance of CART alongside RF and SVM. The results indicated that while RF achieved the highest accuracy, CART provided competitive results with a lower computational cost, making it suitable for scenarios where interpretability is crucial. These results are especially important for wetland mapping. The choice of algorithm should be guided by the study, including the landscape's complexity, the need for interpretability, and the available computational resources.

4 Conclusion

Coastal change analysis is significant for wetland management and environmental studies. Coastal areas can change because of climatic changes, anthropogenic activities and natural factors. In this study, object-based classification and post-classification comparison analysis were done. After obtaining the objects from the Landsat 8 LDCM satellite images of the seasons of 2016, these objects were classified using CART. CART showed excellent performance in classifying satellite images of different seasons used in the study. Post classification comparison was then used to determine the changes between the classified images.

The change in the lake area from February to May has been caused by the increase in temperature and evaporation and the decrease in precipitation. A decrease in the lake area was expected due to the increase in temperature and decrease in precipitation from May to August, but the opposite situation has occurred. It has been determined that this situation was caused by natural factors such as soil permeability and anthropogenic activities such as irrigation. There was an increase in precipitation and a decrease in temperature and evaporation from August to November. The lake area was increased as a result of this situation. This research highlights the significance of seasonal monitoring in wetlands, provides a framework for predicting and managing coastal changes in similar ecosystems worldwide.

Conflict of interest

The authors declare that there is no conflict of interest.

Similarity rate (iThenticate): 16 %

References

[1] A. Delen ve F. Balık Şanlı, Nesne tabanlı sınıflandırma yöntemi ile tarımsal ürün deseninin belirlenmesi. TUFUAB IX. Teknik Sempozyumu, Afyonkarahisar, 2017.

[2] M. Gholoobi, A. Tayyebi , M. Taleyi and A. H. Tayyebi, Comparing pixel based and object based approaches ın land use classification ın mountainous areas. International Archives of the Photogrammetry. Remote Sensing and Spatial Information Science.Volume XXXVIII. Part 8. Kyoto. Japan, 2010.

[3] K. Kalkan ve D. Maktav, Nesne tabanlı ve piksel tabanlı sınıflandırma yöntemlerinin karşılaştırılması (IKONOS Örneği). III. Uzaktan Algılama ve Coğrafi Bilgi Sistemleri Sempozyumu, Gebze, 2010.

[4] S. Wang, S. He, J. Wang, J. Li, X. Zhong, J. Cole, E. Kurbanov, and J. Sha, Analysis of Land Use/Cover changes and driving forces in a typical subtropical region of South Africa. Remote Sensing, 15(19), 4823, 2023. https://doi.org/10.3390/rs15194823.

[5] M. Aghababaei, A. Ebrahimi, A. A. Naghipour, E. Asadi, and J. Verrelst, Classification of plant ecological units in heterogeneous semi-steppe rangelands: performance assessment of four classification algorithms. Remote Sensing, 13(17), 3433, 2021. https://doi.org/10.3390/rs13173433.

[6] P. Turissa, N. Bisman, S. Vincentius, K. Dony and M. Hawis, Evaluation methods of change detection of seagrass beds in the waters of Pajenekang and Gusung Selayar. Trends in Sciences, 18(23), 677, 2021. https://doi.org/10.48048/tis.2021.677.

[7] E. E. Tonyaloğlu, N. Erdogan, B. Çavdar, K. Kurtşan, and E. Nurlu, Comparison of pixel and object based classification methods on rapideye satellite image. Turkish Journal of Forest Science, 5(1), 1-11, 2021. https://doi.org/10.32328/turkjforsci.741030.

[8] L. A. Qu, Z. Chen, M. Li, J. Zhi, and H. Wang, Accuracy Accuracy improvements to pixel-based and object-based lulc classification with auxiliary datasets from Google Earth engine. Remote Sensing, 13(3), 453, 2021. https://doi.org/10.3390/rs13030453.

[9] T. Tochamnanvita and W. Muttitanon, Investigation of coastline changes in three provinces of Thailand using remote sensing. The International Archives of Photogrammetry, Remote Sensing and Spatial Information Sciences, 40(8), 1079, 2014. https://doi.org/10.5194/isprsarchives-XL-8-1079-2014.

[10] M. Modi, R. Kumar, G. R. Shankar and T. R. Martha, Land cover change detection using object-based classification technique: a case study along The Kosi River, Bihar. The International Archives of the Photogrammetry Remote Sensing and Spatial Information Sciences, Volume XL-8, ISPRS Technical Commission VIII Symposium, Hyderabad, India, 2014.

[11] H. M. Badjana, J. Helmschrot, P. Selsam, K. Wala, W. A. Flügel, A. Afouda, and K. Akpagana, Land cover changes assessment using object-based image analysis in the Binah River watershed (Togo and Benin). Earth and Space Science, 2(10), 403-416, 2015. https://doi.org/10.1002/2014EA000083.

[12] E. Sánchez-García, J. E.Pardo-Pascual, A. Balaguer-Beser, and J. Almonacid-Caballer, Analysis of the shoreline Position Extracted from Landsat TM and ETM+ Imagery. The International Archives of Photogrammetry, Remote Sensing and Spatial Information Sciences, 40(7), 991, 2015. https://doi.org/10.5194/isprsarchives-XL-7-W3-991-2015.

[13] X. Lin, Y. Cheng, G. Chen, W. Chen, R. Chen, D. Gao D, Y. Zhang, and Y. Wu, Semantic segmentation of China's coastal wetlands based on Sentinel-2 and Segformer. Remote Sensing, 15(15), 3714, 2023. https://doi.org/10.3390/rs15153714.

[14] A. Gonzalez-Perez, A. Abd-Elrahman, B. Wilkinson, D. J. Johnson, and R. R. Carthy, Deep and machine learning image classification of coastal wetlands using unpiloted aircraft system multispectral images and lidar datasets. Remote Sensing, 14(16), 3937, 2022. https://doi.org/10.3390/rs14163937.

[15] R. Zhou, C. Yang, E. Li, X. Cai, J. Yang, and Y. Xia, Object-based wetland vegetation classification using multi-feature selection of unoccupied aerial vehicle RGB imagery. Remote Sensing, 13(23), 4910, 2021. https://doi.org/10.3390/rs13234910.

[16] S. Adeli, B. Salehi, M. Mahidanpari, and L. J. Quackenbush, Toward a multi-source remote sensing wetland inventory of the USA: preliminary results on wetland inventory of Minnesota. ISPRS annals of the photogrammetry remote sensing and spatial information sciences, 3, 97-100, 2021. https://doi.org/10.5194/isprs-annals-V-3-2021-97-2021.

[17] M. H. Kesikoglu, U. H. Atasever, F. Dadaser-Celik, and C. Ozkan, Performance of ANN, SVM and MLH techniques for land use/cover change detection at Sultan Marshes wetland, Turkey. Water Science and Technology, 80(3), 466-77, 2019. https://doi.org/10.2166/wst.2019.290.

[18] O. O. Festus, W. Ji, and O. A. Zubair, Characterizing the landscape structure of urban wetlands using terrain and landscape indices. Land, 9(1), 29, 2020. https://doi.org/10.3390/land9010029.

[19] H. Ç. Çiftçi, K. Gümüş, and M. G. Gümüş, Analyzing land use and climate change impacts of Suğla water storage in Turkey. Theoretical and Applied Climatology, 155(7), 6797-6814, 2024. https://doi.org/10.1007/s00704-024-05043-0.

[20] T. Feng, H. Ma, and X. Cheng, Land-cover classification of high-resolution remote sensing image based on multi-classifier fusion and the improved Dempster–Shafer evidence theory. Journal of Applied Remote Sensing, 15(1), 014506-014506, 2021. https://doi.org/10.1117/1.JRS.15.014506.

[21] J. P. Simioni, L. A. Guasselli, G. G. De Oliveira, L. F. Ruiz, and G. De Oliveira, A comparison of data mining techniques and multi-sensor analysis for inland marshes delineation. Wetlands Ecology and Management, 28(4), 577-594, 2020. https://doi.org/10.1007/s11273-020-09731-2.

[22] M. Mahdianpari, B. Brisco, J. E. Granger, F. Mohammadimanesh, B. Salehi, S. Banks, S. Homayouni, L. Bourgeau-Chavez, and Q. Weng, The second generation Canadian wetland inventory map at 10 meters resolution using Google Earth Engine. Canadian Journal of Remote Sensing, 46(3), 360-375, 2020. https://doi.org/10.1080/07038992.2020.1802584.

[23] S. Gxokwe, T. Dube, and D. Mazvimavi, Leveraging Google Earth Engine platform to characterize and map small seasonal wetlands in the semi-arid environments of South Africa. The Science of the Total Environment, 803, 150139, 2022. https://doi.org/10.1016/j.scitotenv.2021.150139.

[24] F. Büyükdeveci, Türkiye'nin Doğu Akdeniz kıyısında bulunan Ağyatan (Hurma Boğazı) lagününde yakalanan türlerin av kompozisyonu ve av verimi. Journal of Anatolian Environmental and Animal Sciences, 8(3), 559-567, 2023. https://doi.org/10.35229/jaes.1350126.

[25] M. A. Çelik, Y. Kızılelma, A. E. Gülersoy, ve M. Denizdurduran, Farklı uzaktan algılama teknikleri kullanılarak aşağı Seyhan ovası güneyindeki sulak alanlarda meydana gelen değişimin incelenmesi (1990-2010). Electronic Turkish Studies, 8(12), 263-284, 2013.

[26] United States Geological Survey (USGS), EarthExplorer. https://earthexplorer.usgs.gov/, Accessed 13 March 2017.

[27] United States Geological Survey (USGS), What are the band designations for the Landsat satellites? http://landsat.usgs.gov/band_designations_landsat_satellites.php, Accessed 13 March 2017.

[28] Ç. Göksel, R. M. David, and A. O. Dogru, Environmental monitoring of spatio-temporal changes in northern Istanbul using remote sensing and GIS. International Journal of Environment and Geoinformatics, 5(1), 94-103, 2018. https://doi.org/10.30897/ijegeo.410943.

[29] C. Witharana, and D. L. Civco, Optimizing multi-resolution segmentation scale using empirical methods: Exploring the sensitivity of the supervised discrepancy measure Euclidean distance 2 (ED2). ISPRS Journal of Photogrammetry and Remote Sensing, 87, 108-121, 2014. https://doi.org/10.1016/j.isprsjprs.2013.11.006.

[30] M. H. Kesikoglu, U. H. Atasever, C. Ozkan, and E. Besdok, The usage of rusboost boosting method for classification of impervious surfaces. The International Archives of the Photogrammetry, Remote Sensing and Spatial Information Sciences, 41, 981-985, 2016. https://doi.org/10.5194/isprs-archives-XLI-B7-981-2016.

[31] P. Z. Firouzabadi and E. Ghanavati, Digital approaches for change detection in urban environment, Geographical Research, 22(1), 84, 133-146, 2007.

[32] M. H. Kesikoğlu, Ü. H. Atasever, and C. Özkan, Unsupervised change detection in satellite images using fuzzy c-means clustering and principal component analysis. The International Archives of the Photogrammetry, Remote Sensing and Spatial Information Sciences, 40, 129-132, 2013. https://doi.org/10.5194/isprsarchives-XL-7-W2-129-2013.

[33] L. Bruzzone, and D.Prieto, Automatic analysis of the difference image for unsupervised change detection. IEEE Transactions on Geoscience and Remote sensing, 38(3), 1771-1182, 2000.

[34] F. Pacifici, F. D. Frate, C. Solimini, and W. Emery, An innovative neural-net method to detect temporal changes in high-resolution optical satellite imagery. IEEE Transactions on Geoscience and Remote Sensing, 45(9), 2940–2952, 2007. https://doi.org/10.1109/TGRS.2007.902824.

[35] Climate Data, İklim Karataş (Türkiye). https://tr.climate-data.org/location/26497/, Accessed 20 May 2017.

[36] F. Mohseni, M. Amani, P. Mohammadpour, M. Kakooei, S. Jin, and A. Moghimi, Wetland mapping in great lakes using Sentinel-1/2 time-series imagery and DEM data in Google Earth Engine. Remote Sensing, 15(14), 3495, 2023. https://doi.org/10.3390/rs15143495.

[37] X. B. Tran, V. Vambol, and T. D. Luu, Assessing forest cover changes in Dak Lak province (Central Highlands of Vietnam) from multi-temporal Landsat data and machine learning techniques. Ecological Questions, 35(3), 1-18. https://doi.org/10.12775/EQ.2024.035.

[38] T. K. Oo, N. Arunrat, S. Sereenonchai, A. Ussawarujikulchai, U. Chareonwong, and W. Nutmagul, Comparing four machine learning algorithms for land cover classification in gold mining: A case study of Kyaukpahto Gold Mine, Northern Myanmar, Sustainability, 14(17), 10754, 2022. https://doi.org/10.3390/su141710754.

[39] S. Aldiansyah, and R. A. Saputra, Comparison of machine learning algorithms for land use and land cover analysis using Google Earth engine (Case study: Wanggu watershed). International Journal of Remote Sensing and Earth Sciences, 19(2), 197-210, 2023.

[40] C. U. Rahayu, I. Indarto, and B. E. Cahyono, Using sentinel and comparing two classification algorithms for land cover mapping in the area dominated by small scale heterogeneous agricultural land. IOP Conference Series: Earth and Environmental Science, Bristol, UK, 2022.